

# Unsupervised Segmentation of Synthetic Aperture Radar Sea Ice Imagery Using a Novel Markov Random Field Model

Huawu Deng, *Member, IEEE*, and David A. Clausi, *Senior Member, IEEE*

**Abstract**—Environmental and sensor challenges pose difficulties for the development of computer-assisted algorithms to segment synthetic aperture radar (SAR) sea ice imagery. In this research, in support of operational activities at the Canadian Ice Service, images containing visually separable classes of either ice and water or multiple ice classes are segmented. This paper uses image intensity to discriminate ice from water and uses texture features to identify distinct ice types. In order to seamlessly combine image spatial relationships with various image features, a novel Bayesian segmentation approach is developed and applied. This new approach uses a function-based parameter to weight the two components in a Markov random field (MRF) model. The devised model allows for automatic estimation of MRF model parameters to produce accurate unsupervised segmentation results. Experiments demonstrate that the proposed algorithm is able to successfully segment various SAR sea ice images and achieve improvement over existing published methods including the standard MRF-based method, finite Gamma mixture model, and K-means clustering.

**Index Terms**—Classification, cooccurrence probabilities, expectation-maximization (EM), Gamma distribution, intensity, K-means clustering, Markov random field (MRF), mixture model, pattern recognition, sea ice, segmentation, synthetic aperture radar (SAR), texture, unsupervised.

## I. INTRODUCTION

THE POLAR regions are now being recognized to be of an increasing significance in both economics and environment. A major research initiative on the polar regions is to obtain timely information on the distribution and dynamics of sea ice [1], [2]. The most important tool is satellite-based synthetic aperture radar (SAR) systems. As an important aspect of measurement, monitoring and understanding of sea ice evolution during the seasons, the generation of ice maps is a fundamental step in interpretation of these data. The Canadian Ice Service (CIS) (<http://www.cis.ec.gc.ca/>) is a government agency that generates daily maps for monitoring ice-infested regions. Currently, all of the ice map generation is performed manually using digital techniques. An example of an ice map completed using the World Meteorological Organization (WMO) standard is found in [3]. A primary source of digital imagery in support of CIS operations is RADARSAT, a Canadian SAR satellite.

Manuscript received February 27, 2004; revised September 8, 2004. This work was supported in part by Geomatics for Informed Decisions (GEOIDE), a Natural Sciences and Engineering Research Council (NSERC) Networks of Centres of Excellence and in part by Cryosphere System in Canada (CRYSYS).

The authors are with the Department of Systems Design Engineering, University of Waterloo, Waterloo, ON N2L 3G1, Canada (e-mail: h2deng@engmail.uwaterloo.ca; dclausi@engmail.uwaterloo.ca).

Digital Object Identifier 10.1109/TGRS.2004.839589

Automated segmentation techniques are expected to improve throughput, reduce costs and reduce human bias; however, no computer-assisted method has been proven to be sufficiently robust to support CIS operations.

Computer-assisted SAR sea ice segmentation techniques have not been successful operationally for numerous reasons. SAR sea ice imagery is complex due to both sensor (e.g., speckle noise, antenna gain patterns) and environmental (e.g., ice type transitions, prevailing weather conditions) characteristics. The research in this paper will focus on two particular SAR sea ice segmentation problems. Operationally, analysts need to calculate the ice concentration in SAR images containing both ice and open water. As well, ice regions need to be segmented into regions containing consistent ice types.

A commonly used strategy for segmenting digital imagery will be employed here. First, a method to generate features that uniquely identify the same-content regions as well as differentiate different-content regions is selected. Then, a technique is selected that can group the features into unique classes to produce an appropriate segmentation. With regards to image feature selection, this paper uses image intensity (i.e., tone) to discriminate ice from water regions and uses texture features combined with image intensity to identify ice type regions. If intensity and texture can not distinguish the classes, then additional features are required. This paper does not dwell on using any additional features, but only focuses on using existing intensity and texture models in a new MRF segmentation model.

A common SAR segmentation method in the research literature is the use of thresholding. The dynamic thresholding algorithm proposed by Haverkamp *et al.* [4] first chooses thresholding values from local regions and then thresholds the entire image. As it accounts for the local variance in an image, it meets success in segmenting the sea ice images which have an obviously bimodal gray-level distribution. Soh *et al.* also recognize that the method is based on global appearance, instead of feature-level homogeneity [5]. There are some other segmentation methods which have potential to segment SAR sea ice images. The finite Gamma mixture model was originally applied by Samadani [6] to estimate proportions of ice types in a SAR image. The method uses a mixture model based on assuming a Gamma distribution for each of the ice classes and uses an iterative method to estimate the parameters of the distribution function. The K-means clustering method [7] can be used to cluster feature vectors and generate image segmentations. The weakness of these three methods is that they ignore the spatial relationship of the image pixels which leads to increased sensitivity to image noise, increasing the error rate.

A Markov random field (MRF) is recognized to be a powerful stochastic tool used to model the joint probability distribution of the image pixels in terms of local spatial interactions [8]–[10]. MRF models can be used not only to extract texture features from image textures but also to model the image segmentation problem [10]. Using MRF models for image segmentation has two advantages. First, the spatial relationship can be seamlessly integrated into a segmentation procedure. Second, the MRF-based segmentation model can be inferred in the Bayesian framework which is able to utilize different types of image features.

There are various MRF-based segmentation models that have been developed [11]–[16]. The MRF-based segmentation method has also been applied to segment SAR urban/rural images [17]–[19] using only intensity as a feature. However, the application of MRF models to segment SAR sea ice imagery is not commonly represented in the research literature. Such an application should not use only tone as a feature, but should also incorporate texture. A notable recent paper is the work by Clausi and Yue that studied the relative ability of cooccurrence probabilities and MRF's for SAR sea ice image segmentation [20]. A problem of the available MRF models is that the segmentation performance is highly dependent on the representability of the MRF parameters estimated from features in an image. Due to the within-class variability and nonstationarity of SAR sea ice characteristics, the usual MRF-based segmentation models are unable to properly perform segmentation. A practical MRF-based segmentation model should be able to utilize different types of image features for different segmentation tasks [21].

A standard MRF model is used as a basis for the development here [10] and will be improved on for the purpose of segmenting SAR sea ice imagery. The standard model consists of two components: a region labeling component and a feature modeling component. The region labeling component imposes a homogeneity constraint on the image segmentation process, while the feature modeling component functions to fit the feature data. In the standard model, a constant weighting parameter is used to combine the two components. This model works effectively if training data are available to estimate the parameters of both components. Due to the highly variable nature of the same class features in SAR imagery, training data are inappropriate and, for operational purposes, unsupervised approaches are advocated. As a result, the segmentation procedure should have the ability to learn its parameters without human intervention. In an unsupervised environment, the standard MRF model is unable to work consistently. This is caused by the constant weighting parameter, which is not able to achieve a proper balance between the two components in the entire segmentation procedure.

A new and robust implementation scheme is used here [22] to combine the two components by introducing a variable weighting parameter between the two components. The variable parameter first functions as learning approximately globally optimal parameters. A balance is then achieved between the two components such that the spatial relationship information can be taken into account to refine the parameters when using a simulated annealing scheme for optimization [9]. This approach is demonstrated to eventually generate more accurate SAR sea ice segmentation results than the model with a constant parameter.

The rest of the paper is organized as follows. Section II describes the necessary image features. Section III discusses the inference of a traditional MRF-based segmentation model for using image features and Section IV discusses how to implement the novel segmentation model. Section V presents SAR sea ice image experiments comparing four different methodologies. Conclusions are drawn in Section VI.

## II. FEATURE REPRESENTATION

### A. Image Intensity

SAR backscatter in sea ice imagery depends on the surface roughness as well as the dielectric constant of sea ice or open water. Multiyear ice has a relatively low dielectric constant because of its near zero salinity, and the volume backscattering (reflection off bubbles and sediment within the ice) makes the multiyear ice appear relatively bright in SAR imagery. First-year smooth ice appears dark because it is more saline and has a higher dielectric constant that prevents radar energy from penetrating the ice surface causing the signal to reflect away from the sensor. First-year rough ice appears brighter and often textured due to the uneven surface which causes scattering in many directions.

The backscatter (represented by gray tone) in SAR imagery plays an important role in visual interpretation of sea ice images. However, algorithms based only on tonal statistics have been demonstrated to have poor separation for different ice types [23]. This poor ice type separation is primarily caused by tremendous within-class gray tone variation due to surface roughness as well as the existence of ridges, rubble, rims, and deformation resulting from compression forces [24], [25]. Some success has been met when using variation as a texture after filtering [26], but the improvement is marginal [27]. As open water in seas has a significantly larger dielectric constant than the ice-infected regions, most of the incident radar energy is reflected (not backscattered) so that the SAR image in calm open water areas looks much darker than the ice regions. For partition of ice regions from calm water regions, therefore, the image intensity is strongly advocated.

A significant problem in segmenting SAR sea ice imagery is speckle noise. The speckle noise is visually recognized as an increased frequency of light and dark pixels in what should be a relatively homogeneous gray-level field. Speckle reduction filters [28] can be used to postfilter SAR images; however, these methods tend to blur the boundaries between ice types. A general method to reduce speckle noise is to use multiple looks or noncoherent integration which processes separate portions of an aperture and recombining these portions so that interference does not occur [29], [30]. The speckle-reduced sea ice image is however not constant-pieceswise but generally has pixel values that are Gamma distributed [6], [31]. Denote the site of a pixel in an image by  $s$  and the gray value of the pixel  $s$  by  $x_s$  and the label of  $s$  by  $y_s$ . The Gamma distribution of  $x_s$  with respect to the mean  $\mu_m$  of all pixels belonging to the  $m$ th class is [6]

$$p(x_s | y_s = m) = \frac{l^l}{\mu_m^l (l-1)!} x_s^{l-1} \exp\left(-\frac{l}{\mu_m} x_s\right) \quad (1)$$

where  $l$  denotes the number of looks. Note that this distribution function does not account for any spatial relationship information for the pixel values of ice/water. In Section III, the integra-

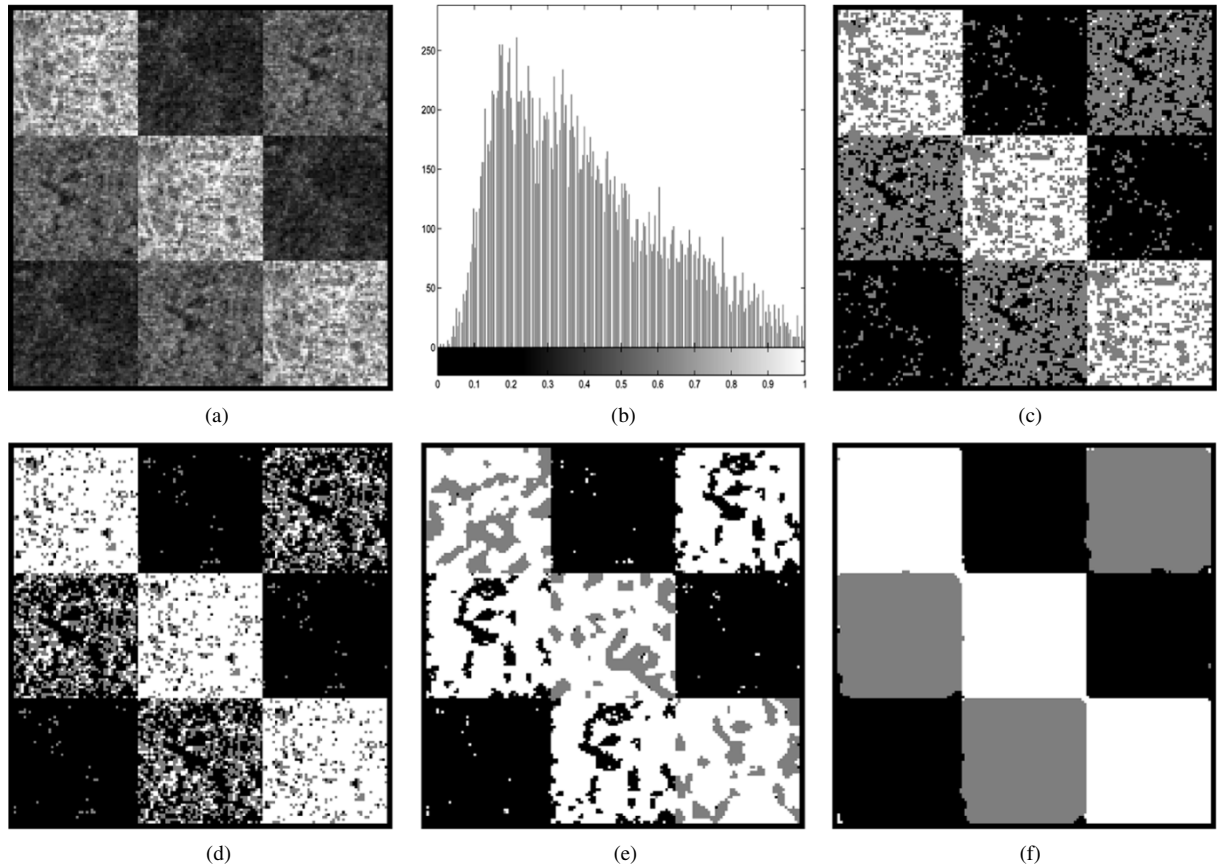


Fig. 1. (a) Checkerboard image with three ice classes: multiyear, gray, and gray-white ice in raster order. (b) Histogram. Intensity-based segmentation using (c) K-means (75.8% accuracy), (d) Gamma mixture model (73.0%), (e) MRF model with  $\alpha = 8$  (68.2%), and (f) MRF model with  $\alpha(i) = 80 * 0.95^i + 1$  (99.3%).

tion of this Gamma distribution into an MRF-based segmentation model will be explored as a means to perform segmentation based on intensity only.

### B. Texture Features

Texture is a very important cue in the human visual system. Texture features have a demonstrated ability to support image segmentation in many areas [32] and have also demonstrated potential for classifying sea ice types in SAR imagery [5], [33]–[35]. Various texture methods are found in the research literature to extract texture features [32]. For SAR sea ice image classification, there is supportive evidence that the gray-level cooccurrence probability (GLCP) method [36] is an effective method to generate appropriate texture features [5], [25], [33]–[35], [37].

Originally proposed by Haralick *et al.* [36], the GLCP method involves determining cooccurring probabilities of all pairwise combinations of gray levels  $(i, j)$  in a fixed-size spatial window as a function of interpixel distance  $(\delta)$  and orientation  $(\theta)$ . The window size determines the ability to capture texture features at different spatial extents. Gray-level quantization is normally performed to accelerate calculation of the GLCP features and to reduce the effects of noise but, at the same time, texture information is reduced [33].

Statistics are applied to the cooccurring probabilities to generate texture features. Generally, these statistics identify some structural aspect of the arrangement of cooccurring probabilities stored within a matrix indexed on  $i$  and  $j$ , which in turn reflects some qualitative characteristic of the local image texture

(e.g., smoothness or roughness). There are a number of statistics that can be used; however, only three statistics are advocated for shift-invariant classification (using pure texture samples), since these should generate preferred discrimination with the least redundancy [35]. Recommended statistics include contrast, entropy, and correlation [33].

Although the GLCP method is assumed to capture consistent feature measurements for the same class regions in an image, the natural variation of the ice classes causes variation in their feature response. Generally, the feature response can be modeled by a Gaussian distribution function. Even if the distribution of feature data is not exactly a Gaussian distribution, the Gaussian function can still be used to approximate it, since a unimodal distribution (i.e., a distribution with a central tendency) is expected. Denote the feature vector extracted from a random image  $(X = x)$  by  $F = f$ , where  $F$  denotes a random variable and  $f$  is an instance of  $F$ .  $Y = y$  stands for a segmented result based on the feature vector  $F = f$ , i.e.,

$$p(f_s^k | y_s = m) = \frac{1}{\sqrt{2\pi\sigma_m^k{}^2}} \exp \left[ -\frac{(f_s^k - \mu_m^k)^2}{2\sigma_m^k{}^2} \right] \quad (2)$$

where  $\mu_m^k$  and  $\sigma_m^k$  are the mean and standard deviation for the  $m$ th class in the  $k$ th feature component, and  $f_s^k$  is the  $k$ th feature component of  $f$  at site  $s$ . In the next section, the Gaussian distribution will be integrated into an MRF-based segmentation model.

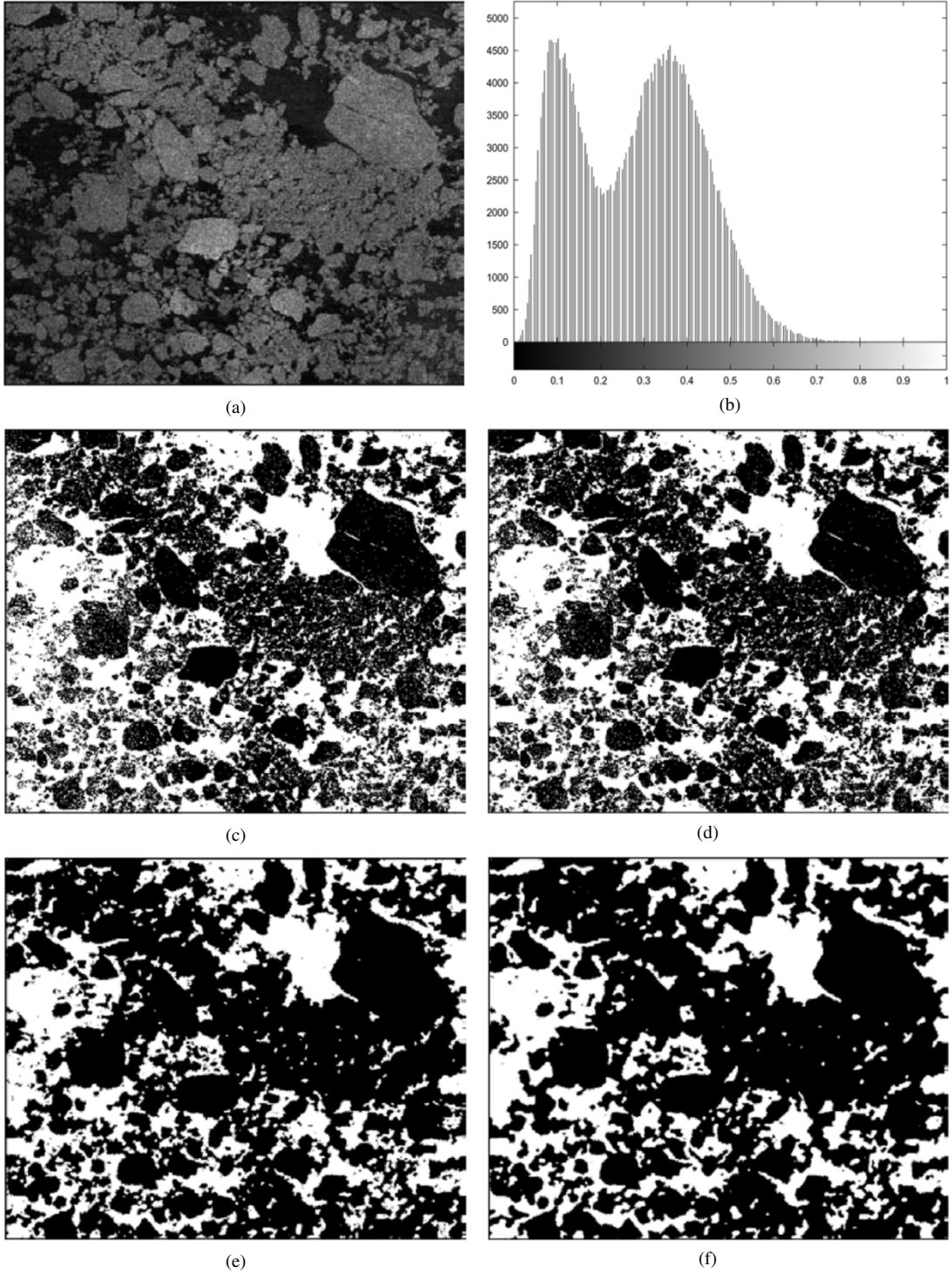


Fig. 2. (a) SAR sea ice image of Baffin Bay/Davis Strait region ( $530 \times 624$  pixels). (b) Histogram. Intensity-based segmentation using (c) K-means, (d) Gamma mixture model, (e) MRF model with  $\alpha = 8$ , and (f) MRF model with  $\alpha(i) = 80 * 0.95^i + 1$ .

### III. SEGMENTATION MODEL

The segmentation problem can be expressed in the Bayesian framework. According to the Bayes rule, the segmentation problem is formulated as

$$P(Y = y | F = f) = \frac{p(F = f | Y = y)P(Y = y)}{p(F = f)}. \quad (3)$$

$P(Y = y | F = f)$  is the *posteriori* probability of  $Y = y$  conditioned on  $F = f$ .  $p(F = f | Y = y)$  denotes the probability distribution of  $F = f$  conditioned on  $Y = y$  and functions to fit the feature data, which is thus referred to as the feature modeling component.  $P(Y = y)$  is a *priori* probability of  $Y = y$  and is used to describe the label distribution of a segmented result only, which is normally referred to as the region labeling component.  $p(F = f)$  is the probability distribution of  $F = f$ .

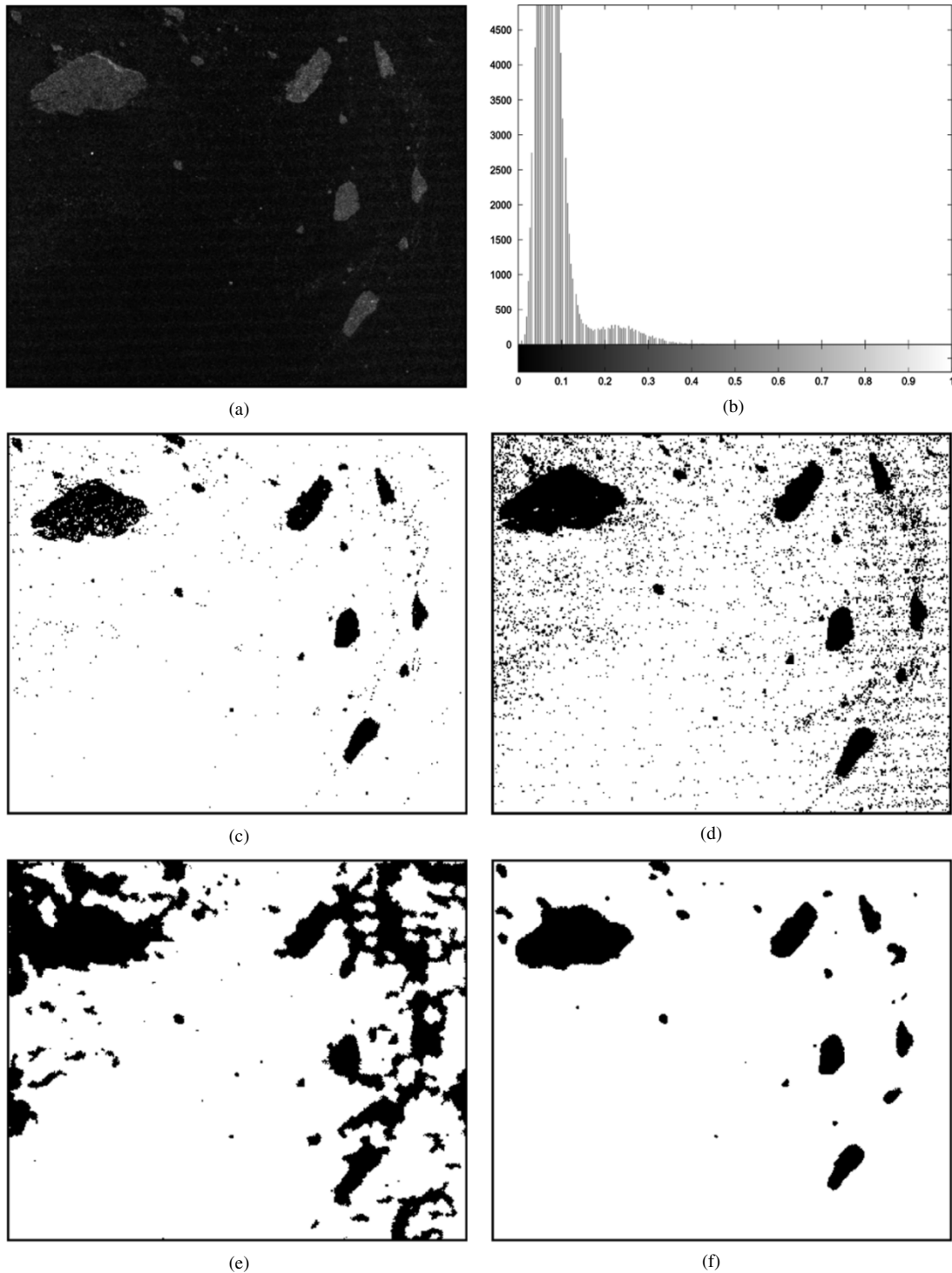


Fig. 3. (a) SAR sea ice image of Baffin Bay/Davis Strait region ( $417 \times 330$  pixels). (b) Histogram. Intensity-based segmentation using (c) K-means, (d) Gamma mixture model, (e) MRF model with  $\alpha = 8$ , and (f) MRF model with  $\alpha(i) = 80 * 0.95^i + 1$ .

A few assumptions are required to derive an MRF-based segmentation model. *The first assumption is that each component of  $F = f$  be independent on the other components with respect to  $Y = y$  (conditional independence)*. Suppose there are  $K$  components in the feature vector  $f = \{f^k | k = 1, 2, \dots, K\}$ . Equation (3) is then transformed into

$$P(Y = y | F = f) = \frac{\prod_{k=1}^K [p(f^k | Y = y)] P(Y = y)}{p(F = f)} \quad (4)$$

where  $p(f^k | Y = y)$  stands for the probability distribution of the extracted feature component  $f^k$  conditioned on the segmented result  $Y = y$ . As  $F = f$  is known and only the relative probability is of concern when maximizing  $P(Y = y | F = f)$ ,  $p(F = f)$  does not vary with respect to any solution  $Y = y$  and hence the denominator can be disregarded.

Suppose the energy form of  $P(Y = y)$  is  $E_R$  and that of  $\prod_{k=1}^K [p(f^k | Y = y)]$  is  $E_F$ . A general energy form  $E$

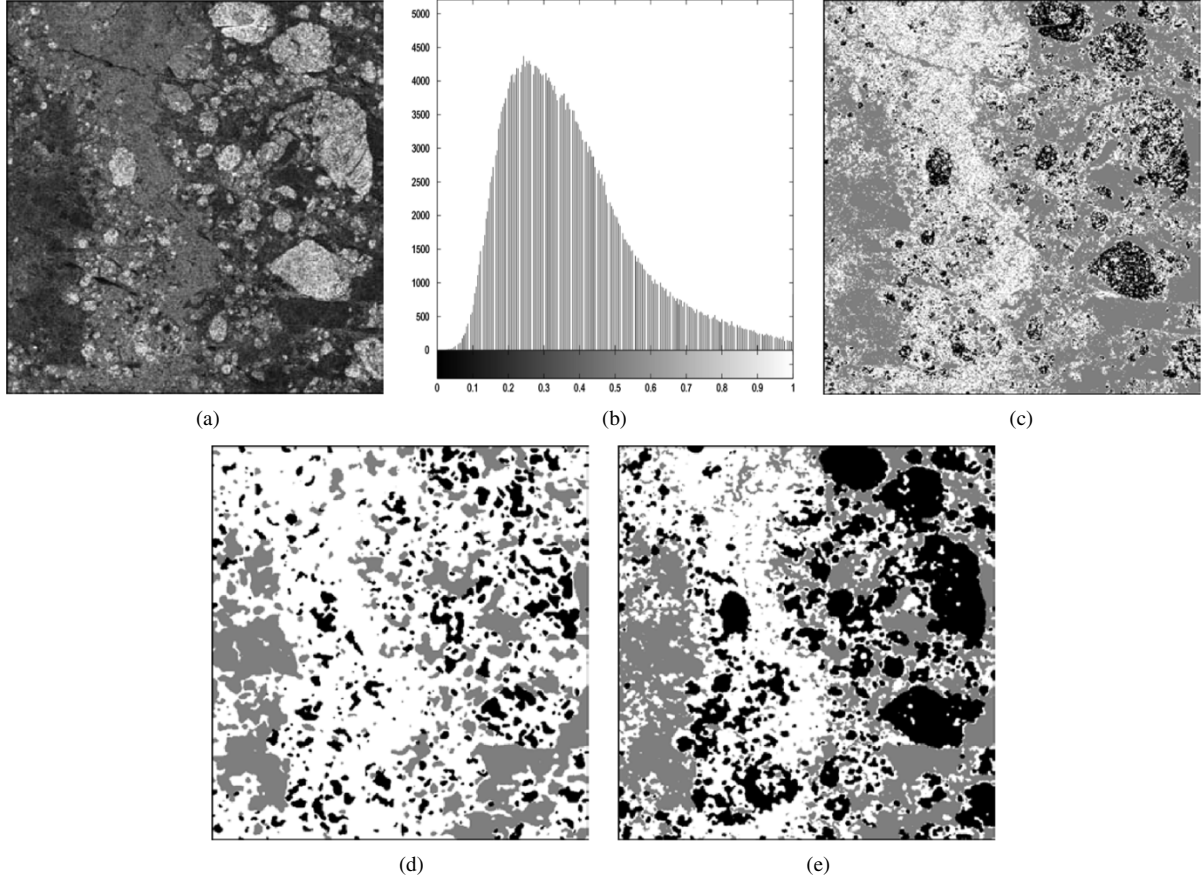


Fig. 4. (a) SAR image ( $631 \times 595$  pixels, Baffin Bay/Davis Strait region). (b) Histogram. Segmentation using (c) K-means, (d) MRF model with  $\alpha = 8$ , and (e) MRF model with  $\alpha(i) = 80 * 0.95^i + 1/9$ . All segmentations performed using both the intensity feature fused with GLCP texture features.

for  $P(Y = y | F = f)$  can be derived from the product of  $P(Y = y)$  and  $\prod_{k=1}^K [p(f^k | Y = y)]$

$$E = E_R + \alpha E_F \quad (5)$$

where  $\alpha$  is a weighting parameter used to determine how much  $E_R$  and  $E_F$  individually contribute to the entire energy  $E$  [38], [39]. Most of the available two-component MRF models normally assumes  $\alpha = 1$  [9]. Its Gibbs form [10] is  $P(Y = y | F = f) = (1/Z) \exp[-(1/T)E]$ , where  $Z = \sum_{\Omega_Y} \exp[-(1/T)E]$ , and  $\Omega_Y$  is a set of all possible configurations of  $Y$ .

Concrete forms for each of  $E_R$  and  $E_F$  are required for practical segmentation. Often, MRF-based segmentation models use the multilevel logistic (MLL) model for modeling the label distribution. For a segmentation task, the second-order pairwise MLL model is generally chosen and the potentials of all non-pairwise cliques are defined to be zeros [10]. The energy of the pairwise MLL model is as follows:

$$E_R(y) = \sum_s \left[ \beta \sum_{t \in N_s} \delta(y_s, y_t) \right] \quad (6)$$

where  $\delta(y_s, y_t) = -1$  if  $y_s = y_t$ ,  $\delta(y_s, y_t) = 1$  if  $y_s \neq y_t$ ,  $\beta$  is a constant which can be specified *a priori*, and  $N_s$  represents the neighborhood centered on  $s$  [9].  $E_R(y)$  denotes the energy of local image regions.

The forms of  $p(f^k | Y = y)$  may be different depending on what features are used. For the task of partitioning ice regions

from water regions, the intensity feature is used as the only one image feature to represent the difference between ice regions and water regions. As indicated in Section II-A, the intensity feature can be modeled using a Gamma distribution, allowing the energy form  $E_F$  of (1) to be written as

$$E_F(x) = \sum_{s, Y_s=m} \left\{ \frac{l}{\mu_m} x_s - (l-1) \log x_s + l \log \mu_m \right\}. \quad (7)$$

For the task of segmenting different ice types, the GLCP features are used as the image features. As indicated in Section II-B, the individual GLCP feature generally can be modeled by a Gaussian distribution. The energy form  $E_F$  of the product of all  $p(f_s^k | Y_s = m)$  can be written as

$$E_F(f) = \sum_{s, Y_s=m} \left\{ \sum_{k=1}^K \left[ \frac{(f_s^k - \mu_m^k)^2}{2(\sigma_m^k)^2} + \log(\sqrt{2\pi}\sigma_m^k) \right] \right\} \quad (8)$$

where  $\mu_m$  and  $\sigma_m$  represent the class mean and standard deviation.

#### IV. IMPLEMENTATION SCHEME

To implement the MRF model (5) requires estimation of four parameters:  $\beta$  [from (6)],  $\alpha$  [from (5)],  $\mu_m$ , and  $\sigma_m$  (for all  $m$ ). Traditionally, estimation of  $\mu_m$  and  $\sigma_m$  for each class requires training data. An unsupervised approach does not allow the use of training data. Instead, the expectation-maximization (EM) algorithm [40], [41] is an iterative method that can be used to

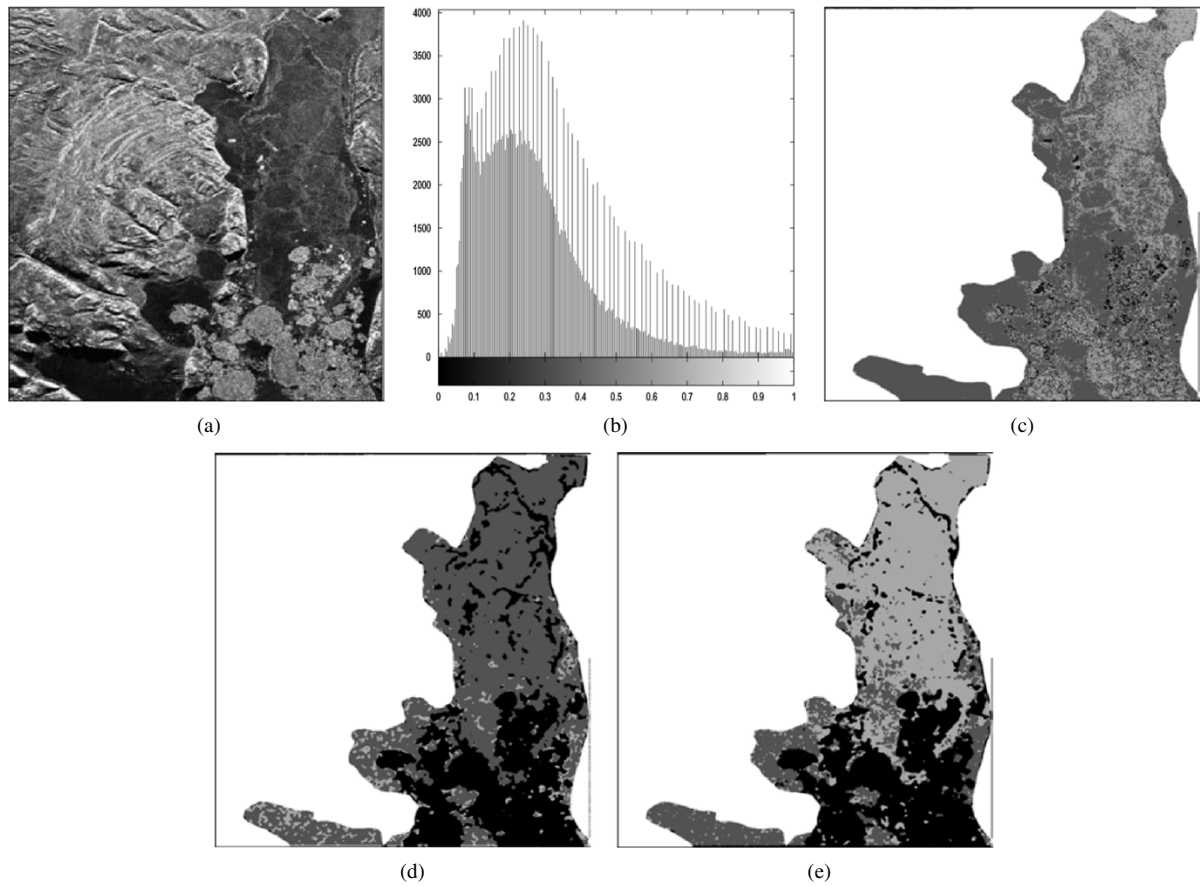


Fig. 5. (a) SAR image ( $864 \times 806$  pixels, Mould Bay region). (b) Histogram. Land areas are masked out for segmentation testing. Segmentation using (c) K-means, (d) MRF model with  $\alpha = 8$ , and (e) MRF model with  $\alpha(i) = 80 * 0.95^i + 1/9$ . All segmentations performed using both the intensity feature fused with GLCP texture features.

estimate  $\mu_m$  and  $\sigma_m$ . In order to avoid the practically impossible calculation of the E-step [18], [41], the EM algorithm is modified for the MRF model (5) as follows.

- 1) A random image segmentation is used for initialization.
- 2) Estimate  $\mu_m$  and  $\sigma_m$  from the feature data  $F = f$  (intensity or GLCP or fused intensity/GLCP features) based on the segmented image

$$\mu_m^k = \frac{1}{N} \sum_{s, Y_s=m} f_s^k$$

$$\sigma_m^k = \left[ \frac{1}{N-1} \sum_{s, Y_s=m} (f_s^k - \mu_m^k)^2 \right]^{\frac{1}{2}}.$$

- 3) Refine the segmentation result based on the estimated  $\mu_m$  and  $\sigma_m$  by minimizing (5) using the Metropolis sampling with a simulated annealing scheme [10].
- 4) Repeat Steps 2) and 3) until a stopping criterion is satisfied.

Steps 2) and 3) are quite similar to the E-step and M-step but are modified for efficiency. The remaining difficulty is that there is no closed-form definition for  $\beta$  and  $\alpha$  in the EM algorithm. A commonly used strategy [9], [17] is to assign *a priori* constant values by experience before executing the EM algorithm. Both parameters  $\beta$  and  $\alpha$  function in the same manner by assigning weights to their corresponding energy components, and hence one of them can be fixed. Here,  $\beta$  is fixed to be 1, and only

$\alpha$  is required to be adjusted. As the weighting parameter  $\alpha$  is normally set as a constant parameter, the segmentation result often falls into three cases.

First, if the constant parameter makes the region labeling component dominant, the values of estimated parameters  $\mu_m$  and  $\sigma_m$  may deviate considerably from the feature data and the segmented result is not consistent. Second, if the constant parameter makes the feature modeling component dominant, spatial relationship information would be ignored in the final segmented result. Third, if a balance can be achieved between both components by choosing a proper constant parameter, the estimated parameters are normally not globally but locally optimal.

A root problem is that the MRF-based segmentation model is very easily trapped in local maxima due to the spatial homogeneity constraint imposed by the region labeling component. As a result, the feature modeling component might not be able to learn the global parameters (i.e.,  $\mu_m$  and  $\sigma_m$  for each class). Stewart *et al.* [39] analyzed the relationship between the two terms in their MRF model in detail and proposed a supervised solution for the weighting parameter (they called it the shape parameter) according to *a priori* information of the size of region shapes. This methodology is not useful for the unsupervised requirement.

A new implementation scheme is proposed here to solve this problem by making the weighting parameter  $\alpha$  vary during unsupervised segmentation. The introduction of the variable weighting parameter should not only enable the segmentation

procedure to learn the global parameters of the feature modeling component but also impose a spatial homogeneity constraint on the label distribution (through the region labeling component). In this context, the parameter may vary with respect to the annealing procedure. The following function is selected for the variable weighting parameter  $\alpha$ :

$$\alpha(i) = c_1 * \gamma^i + c_2, \quad 0 < \gamma < 1 \quad (9)$$

where  $\gamma$ ,  $c_1$ , and  $c_2$  are constants and  $i$  represents the  $i$ th iteration. Experimentally, we have determined that setting  $\gamma = 0.95$ ,  $c_1 = 80$ , and  $c_2 = 1/K$  (where  $K$  is the dimension of the feature space) are appropriate values for a variety of imagery. Using this function, the feature modeling component will first [when  $\alpha(i)$  is larger] dominate the MRF model in order to learn its global parameters and then [when  $\alpha(i)$  is close to  $c_2$ ] interact with the region labeling component to refine the segmented result. Thus, the energy of the MRF model can be rewritten as

$$E = E_R + \alpha(i)E_F. \quad (10)$$

## V. EXPERIMENTAL RESULTS

### A. Testing Methodology

To determine ice concentrations, the intensity feature is the only necessary feature. However, to segment multiple ice images, preferred results are obtained fusing the intensity and the GLCP features. As the Gamma mixture model is based on the distribution of intensity in an image, this method achieved poor results when applied to the multiple ice images and these are not presented here. The other three methods are applied using a fused feature set of intensity and GLCP texture features. Since feature axes have different dimensions, feature space scaling is a necessity. An appropriate method is to scale all of the feature space dimensions to the range [0, 1], and this has been applied to all feature sets.

The parameters for extracting the GLCP features are set as follows. Although classification using pure samples supported the need for three statistics (contrast, entropy, and correlation [33]), our experience (currently unpublished) is that the correlation statistic is a poor choice for segmenting SAR sea ice images due to the misleading features it produces across high contrast texture boundaries. As a result, only two statistics are used here (contrast and entropy), which display appropriate feature values across the numerous high contrast boundaries found in SAR sea ice imagery. The window size is  $7 \times 7$ . One displacement ( $\delta = 1$ ) and four orientations ( $0^\circ$ ,  $45^\circ$ ,  $90^\circ$ ,  $135^\circ$ ) are chosen. Thus, each pixel is represented by an eight-dimensional vector of GLCP features. The quantization level is set to 64.

Four methods are used for image segmentation: 1) the K-means clustering method [7]; 2) the finite Gamma mixture model followed by a maximum-likelihood classification [6]; 3) the traditional MRF model with a constant weighting parameter; and 4) the advanced MRF model with a variable weighting parameter (the method promoted in this paper).

The K-means clustering method stops its iterations when all pixels cease changing labels. The initial seeds for K-means clustering are chosen randomly. Multiple K-means tests using different randomly selected seeds produced similar results. The stopping criterion of implementing the finite Gamma mixture

model occurs when the coefficient of each class changes less than one percentage (1%). The two MRF segmentation methods are implemented using the modified EM algorithm, discussed in Section IV. A fixed number of iterations is used as the stopping criterion in all experiments. Testing indicated that the segmentation results will not change appreciably after 150 iterations and the result at the 150th iteration can be considered as final. The following represents pseudocode to implement the modified EM algorithm for the proposed MRF model.

```

Create an initial image segmentation using random labels (Y);
for i = 1:150
    Estimate  $\mu$  and  $\sigma$  for each class given the current Y and F;
    Calculate  $\alpha$ :  $\alpha(i) = 80 * 0.95^i + 1/K$ ;
    Calculate  $E_R$  and  $E_F$ ;
    Obtain a new Y given the Metropolis sampler to estimate
        Equation (10) using a simulated annealing scheme [10];
end

```

The simulated annealing scheme is the logarithmic scheme used in [9]. The traditional MRF model also uses the above algorithm but sets  $\alpha(i)$  to be constant. A variety of  $\alpha$  have been tested and the use of  $\alpha = 8$  is found to generate the best average result across all of the test images. Only results using  $\alpha = 8$  are reported.

All four segmentation methods are provided with the number of classes found in the specific image. Five SAR sea ice images are used for testing: one test image with known boundaries, two based on intensity (ice versus no-ice) and two based on texture (ice classification). All test examples use the same parameters for each method.

### B. Known Class Boundaries

To verify the applicability of this new MRF model to the segmentation of SAR sea ice imagery, a test image using SAR sea ice samples with known class boundaries was created [Fig. 1(a)]. Tone-distinct samples of multiyear, gray, and gray-white ice were obtained from the SAR image in Fig. 4. The samples are placed in a  $3 \times 3$  checkerboard pattern. Visually, the boundaries are quite distinct based on local estimates of tone, however, the global histogram demonstrates a unimodal distribution [Fig. 1(b)]. The segmentations in Fig. 1(c)–(f) use only intensity as a feature. K-means [Fig. 1(c)] and the Gamma mixture model [Fig. 1(d)] illustrate ineffective segmentations primarily, since each method does not take into account spatial relationships. The MRF with a constant weighting parameter also generates an ineffective segmentation, with significant regional misclassifications that appear “clumpy.” However, the variable weighting parameter achieves an accurate segmentation result (99.3%) with all boundaries and regions accurately identified [Fig. 1(f)]. This demonstrates that the new model produces improved segmentation performance relative to the traditional model, K-means clustering, and the Gamma mixture model.

### C. Segmentation of Ice and Water Imagery

Two images have been extracted from a larger RADARSAT ScanSAR scene (C-band, HH, 100-m pixel spacing) which

covers Baffin Bay and Davis Strait captured on June 24, 1998. Both of these images show sea ice in open water and the goal is to calculate the ice concentration. The first image is depicted in Fig. 2(a), and its bimodal histogram is shown in Fig. 2(b). The four methods are applied to segment this image based on intensity only. As the pixels of ice and water are separable in the feature space, the finite Gamma mixture model and the K-means clustering method can properly segment ice and water classes, as shown in Fig. 2(c) and (d). Both the MRF model with a constant parameter [Fig. 2(c)] and the MRF model with a variable parameter [Fig. 2(d)] improve the uniformity in the ice and water regions, generating effective segmentations.

Another SAR image requiring an ice concentration calculation is shown in Fig. 3(a). Although a human is readily able to identify the ice regions in this image, the computer-assisted segmentation algorithms generally find this image to be difficult to segment. This image generates a bimodal histogram [Fig. 3(b)], however, the ice concentration is quite low which reduces the number of pixels associated with the ice class. The K-means clustering [Fig. 3(c)] result once again has a fairly good estimate of the ice, however, the segmentation is spotty in both the open water and ice regions. The Gamma mixture model [Fig. 3(d)] performs very poorly and is unable to properly segment the ice from the open water. Also, the MRF model with a constant weighting parameter produces a poor segmentation by overestimating the ice regions [Fig. 3(e)]. The constant weighting parameter forces the region labeling component to contribute less energy to the whole system than the feature modeling component so that the final segmented result does not incorporate sufficient spatial relationship information. The most successful segmentation approach is that obtained using the MRF model with a variable weighting parameter [Fig. 3(f)] which does a more effective job of separating ice and open water and identifying them as uniform regions.

#### D. Segmentation of Multiple Ice Imagery

The image shown in Fig. 4(a) is part of a C-band HH RADARSAT ScanSAR image (100-m pixel spacing) in the Baffin Bay/Davis Strait region acquired on February 7, 1998. This image consists of three types of sea ice: multiyear ice (bright floes), gray-white ice (running primarily from top to bottom in the middle), and gray ice (observed on the left hand side and surrounding the multiyear floes on the right hand side). Visually, this image would be very difficult to segment and even the manual segmentations by trained human operators would have noticeable variability (manual segmentation would also be a very time consuming exercise). Although tonal distinctions are noted visually, the histogram is unimodal [Fig. 4(b)] which leads to failure of segmentation based on intensity alone (for brevity, not shown). As a result, the segmentation is performed using both intensity and texture.

Segmentation using K-means [Fig. 4(c)] shows a segmentation that is not effective. Boundaries of unique regions are somewhat defined, however, the regions themselves are "spotty" in their classification, since local spatial interactions are not accounted. Segmentation using the MRF model with constant weighting produces an ineffective segmentation where the form of the ice regions is not properly recognized [Fig. 4(d)]. The

only method that produces an acceptable segmentation is the MRF model using a variable weighting scheme. Here, the multiyear floes are consistent and the gray and gray-white regions show acceptable divisions. As there is large intensity variance in same-class pixels, the spatial homogeneity constraint on neighboring pixels is very important for clustering the same-class pixels. As a result, the K-means clustering method is unable to properly cluster the three ice types. Also, a proper feature set is very important to differentiate the three ice types. If using only intensity as the image feature, the MRF model with a constant or variable parameter generate more uniform ice type regions (relative to K-means) but fail to properly identify all three ice types. When using only the GLCP features, the result by the MRF model with a constant or variable weighting parameter has some improvement over that by the K-means clustering method, but the means of three ice types are still confused. The application of the MRF model with the variable parameter using a fused (texture and intensity) feature set is able to generate the most accurate result.

The last test image, shown in Fig. 5(a), was used in the work of [42] and [35] for classification testing (X-Band HH STAR-1, 6-m pixel spacing, seven looks, covering Mould Bay, NWT, acquired on March 3, 1984). The land areas are manually masked out. The rest of this image consists of three ice types: multiyear ice (bright floes), first-year smooth ice (dark areas noted primarily near the coastal regions), and first-year rough ice (gray areas noted primarily toward the top half of the image). The image histogram [Fig. 5(b)] is bimodal, but the significant overlap between the two modes forces the distribution to be nearly unimodal in nature. The classes are not well segmented using intensity alone, so a fused feature set of intensity and texture is used. The K-means method is able to segment the first-year smooth ice; however, it is unable to make a distinction between the first-year rough and multiyear ice types [Fig. 5(c)]. The MRF model with constant weighting is able to segment the multiyear ice, but is unable to make a proper distinction between the first-year rough and first-year smooth ice types [Fig. 5(d)]. The only method that is able to properly segment the image is the MRF model using variable weighting [Fig. 5(e)]. Here, all three ice types are well identified and a strong segmentation is achieved.

The algorithm is coded in MATLAB running on a Pentium IV computer (2.0 GHz) and requires approximately 2 h for obtaining the result in Fig. 5(e). MATLAB is notoriously poor with iterative structures and, based on the authors' experience converting other MATLAB programs to C, the solution time would be reduced significantly, probably to the order of minutes.

## VI. CONCLUSION

A new methodology for image segmentation is proposed, developed, and tested successfully for a variety of SAR sea ice imagery. Published methods such as K-means and the Gamma mixture model do not account for spatial interactions and rely only on the feature space representation. However, the MRF models can be formulated to explicitly account for spatial interactions. Unfortunately, the traditional MRF model is unable to dynamically account for region labeling and feature space

interactions. Using a functional-based method, the new methodology dynamically weights these two components in an appropriate manner to generate very strong image segmentations. Images that require calculation of ice concentration are segmented using only intensity as a feature. Instead of using the traditional Gaussian distribution in the MRF model, the MRF models used in this paper incorporate a Gamma distribution, since this is a better model of the ice class intensity distributions. Images requiring segmentation of various ice types required the use of both intensity and texture. The texture features were included in the MRF model by assuming the standard Gaussian distribution. This MRF model using the variable weighting scheme was the only methodology that successfully and consistently segmented all of the test images.

#### ACKNOWLEDGMENT

The authors are thankful to the Canadian Ice Service for providing the SAR sea ice images. All RADARSAT images copyright by the Canadian Space Agency (<http://www.space.gc.ca>).

#### REFERENCES

- [1] D. G. Barber, M. J. Manore, T. A. Agnew, H. Welch, E. D. Soulis, and E. F. LeDrew, "Science issues relating to marine aspects of the cryosphere: Implications for remote sensing," *Can. J. Remote Sens.*, vol. 18, no. 1, pp. 46–55, 1992.
- [2] F. Carsey, "Review and status of remote sensing of sea ice," *IEEE J. Oceanic Eng.*, vol. 14, no. 2, pp. 127–138, Apr. 1989.
- [3] K. Partington, "A data fusion algorithm for mapping sea-ice concentrations from special sensor microwave/imager data," *IEEE Trans. Geosci. Remote Sens.*, vol. 38, no. 4, pp. 1947–1958, Apr. 2000.
- [4] D. Haverkamp, L. K. Soh, and C. Tsatsoulis, "A dynamic local thresholding technique for sea ice classification," in *Proc. IGARSS*, vol. 2, Aug. 18–21, 1993, pp. 638–640.
- [5] L. K. Soh and C. Tsatsoulis, "Texture analysis of SAR sea ice imagery using gray level co-occurrence matrices," *IEEE Trans. Geosci. Remote Sens.*, vol. 37, no. 2, pp. 780–795, Mar. 1999.
- [6] R. Samadani, "A finite mixtures algorithm for finding proportions in SAR images," *IEEE Trans. Image Process.*, vol. 4, no. 8, pp. 1182–1185, Aug. 1995.
- [7] R. O. Duda and P. E. Hart, *Pattern Classification and Scene Analysis*. New York: Wiley, 2000.
- [8] J. E. Besag, "Spatial interaction and the statistical analysis of lattice systems (with discussion)," *J. R. Stat. Soc.*, vol. B-36, pp. 192–236, 1974.
- [9] S. Geman and D. Geman, "Stochastic relaxation, Gibbs distributions, and the Bayesian restoration of images," *IEEE Trans. Pattern Anal. Machine Intell.*, vol. PAMI-6, no. 6, pp. 721–741, Jun. 1984.
- [10] S. Z. Li, *Markov Random Field Modeling in Computer Vision*. New York: Springer-Verlag, 2001.
- [11] F. S. Cohen and D. B. Cooper, "Simple parallel hierarchical and relaxation algorithms for segmenting noncausal Markovian random fields," *IEEE Trans. Pattern Anal. Machine Intell.*, vol. PAMI-9, no. 2, pp. 195–219, Feb. 1987.
- [12] C. S. Won and H. Derin, "Unsupervised segmentation of noisy and textured images using Markov random fields," *Graph. Models Image Process.*, vol. 54, no. 4, pp. 308–328, 1992.
- [13] D. Geman, S. Geman, C. Graffigne, and P. Dong, "Boundary detection by constrained optimization," *IEEE Trans. Pattern Anal. Mach. Intell.*, vol. 12, no. 7, pp. 609–628, Jul. 1990.
- [14] D. K. Panjwani and G. Healey, "Markov random field models for unsupervised segmentation of textured color images," *IEEE Trans. Pattern Anal. Mach. Intell.*, vol. 17, no. 10, pp. 939–954, Oct. 1995.
- [15] S. A. Barker, "Image segmentation using Markov random field models," Ph.D. dissertation, Cambridge Univ., Cambridge, U.K., 1998.
- [16] D. E. Melas and S. P. Wilson, "Double Markov random fields and Bayesian image segmentation," *IEEE Trans. Signal Process.*, vol. 50, no. 2, pp. 357–365, Feb. 2002.
- [17] H. Derin, P. A. Kelly, G. Vezina, and S. G. Labitt, "Modeling and segmentation of speckled images using complex data," *IEEE Trans. Geosci. Remote Sens.*, vol. 28, no. 1, pp. 76–87, Jan. 1990.
- [18] P. A. Kelly, H. Derin, and K. D. Hartt, "Adaptive segmentation of speckled images using a hierarchical random field model," *IEEE Trans. Acoust., Speech, Signal Process.*, vol. 36, no. 10, pp. 1628–1641, Oct. 1988.
- [19] E. Rignot and R. Chellappa, "Segmentation of polarimetric synthetic aperture radar data," *IEEE Trans. Image Process.*, vol. 1, no. 3, pp. 281–300, Jul. 1992.
- [20] D. A. Clausi and B. Yue, "Comparing cooccurrence probabilities and Markov random fields for texture analysis of SAR ice imagery," *IEEE Trans. Geosci. Remote Sens.*, vol. 42, no. 1, pp. 215–228, Jan. 2004.
- [21] P. P. Raghu and B. Yegnanarayana, "Segmentation of Gabor-filtered textures using deterministic relaxation," *IEEE Trans. Image Process.*, vol. 5, no. 12, pp. 1625–1635, Dec. 1996.
- [22] H. Deng and D. A. Clausi, "Unsupervised image segmentation using a simple MRF model with a new implementation scheme," in *Proc. 17th Int. Conf. Pattern Recognition*, vol. 2, 2004, pp. 691–694.
- [23] J. D. Lyden, B. A. Burns, and A. L. Maffett, "Characterization of sea ice types using synthetic aperture radar," *IEEE Trans. Geosci. Remote Sens.*, vol. GE-22, no. 5, pp. 431–439, Sep. 1984.
- [24] E. O. Lewis, B. W. Currie, and S. Haykin, *Detection and Classification of Ice*. New York: Wiley, 1987.
- [25] M. E. Shokr, "Evaluation of second-order texture parameters for sea ice classification from radar images," *J. Geophys. Res.*, vol. 96, no. C6, pp. 10 625–10 640, 1991.
- [26] B. A. Burns, E. S. Kasischke, and D. R. Nuesch, "Extraction of texture information from SAR data: Application to ice and geological mapping," in *Intl. Symp. Remote Sensing Environment*, Fort Worth, TX, 1982, pp. 861–868.
- [27] E. Heolbaek-Hansen, H. Thjelmeland, O. M. Johannessen, T. Olaussen, and R. Karpuz, "Speckle reduction and maximum likelihood classification of SAR images from sea ice recorded during MIZEX 87," in *Proc. IGARSS*, vol. 2, Vancouver, BC, Canada, 1988, pp. 755–758.
- [28] A. Lopes, E. Nezry, R. Touzi, and H. Laur, "Structure detection and statistical adaptive speckle filtering in SAR images," *Int. J. Remote Sens.*, vol. 14, no. 9, pp. 1735–1758, 1993.
- [29] E. S. Kasischke, G. A. Meadows, and P. L. Jackson, *The Use of Synthetic Aperture Radar to Detect Hazards to Navigation*. Ann Arbor, MI: Environ. Res. Inst. Michigan, 1984.
- [30] J. S. Lee, "Speckle analysis and smoothing of synthetic aperture radar images," *Comput. Graphics Image Process.*, vol. 17, pp. 24–32, 1981.
- [31] J. S. Lee and I. Jurkevich, "Segmentation of SAR images," *IEEE Trans. Geosci. Remote Sens.*, vol. 27, no. 6, pp. 674–680, Nov. 1989.
- [32] M. Tuceryan and A. K. Jain, "Texture analysis," in *Handbook of Pattern Recognition and Computer Vision*, Singapore: World Scientific, 1993, ch. 2.
- [33] D. A. Clausi, "An analysis of co-occurrence texture statistics as a function of grey level quantization," *Can. J. Remote Sens.*, vol. 28, no. 1, pp. 1–18, 2002.
- [34] —, "Comparison and fusion of co-occurrence, Gabor and MRF texture features for classification of SAR sea-ice imagery," *Atmos.-Ocean*, vol. 39, no. 3, pp. 183–194, 2000.
- [35] D. G. Barber and E. F. LeDrew, "SAR sea ice discrimination using texture statistics: A multivariate approach," *Photogramm. Eng. Remote Sens.*, vol. 57, no. 4, pp. 385–395, 1991.
- [36] R. M. Haralick, K. Shanmugam, and I. Dinstein, "Textural features for image classification," *IEEE Trans. Syst., Man, Cybern.*, vol. SMC-3, pp. 610–621, 1973.
- [37] A. Baraldi and F. Parmiggiani, "An investigation of the textural characteristic associated with gray level cooccurrence matrix statistical parameters," *IEEE Trans. Geosci. Remote Sens.*, vol. 33, no. 2, pp. 293–304, Mar. 1995.
- [38] P. C. Smits and S. G. Dellepiane, "Discontinuity-adaptive Markov random field model for the segmentation of intensity of SAR images," *IEEE Trans. Geosci. Remote Sens.*, vol. 37, no. 1, pp. 627–631, Jan. 1999.
- [39] D. Stewart, D. Blacknell, A. Blake, R. Cook, and C. Oliver, "Optimal approach to SAR image segmentation and classification," in *Proc. Inst. Elect. Eng.—Radar, Sonar Navig.*, vol. 147, 2000, pp. 134–142.
- [40] A. P. Dempster, N. M. Laird, and D. B. Rubin, "Maximum likelihood from incomplete data via the EM algorithm," *J. R. Stat. Soc.*, vol. B-1, pp. 1–38, 1977.
- [41] J. Zhang, "The mean field theory in EM procedures for Markov random fields," *IEEE Trans. Signal Process.*, vol. 40, no. 10, pp. 2570–2583, Oct. 1992.
- [42] A. D. Nichols, J. W. Wilhem, T. W. Gaffield, R. D. Inkster, and S. K. Leung, "A SAR for real-time ice reconnaissance," *IEEE Trans. Geosci. Remote Sens.*, vol. GE-24, no. 3, pp. 383–389, May 1986.



**Huawu Deng** (M'03) received the B.A.Sc. degree from Beijing University, Beijing, China, in 1992, the M.Eng. degree from the Research Institute of Petroleum Exploration and Development, Beijing, China, in 1995, and the Ph.D. from Nanyang Technological University, Singapore, in 2001.

From 2000 to 2002, he was an Information Technology Analyst for a regional bank in Singapore. He is currently a Postdoctoral Research Fellow with the University of Waterloo, Waterloo, ON, Canada. His current research interests are in image processing (texture modeling, image classification, image segmentation, image retrieval), computer vision, pattern recognition, and remote sensing data analysis.



**David Clausi** (S'93–M'96–SM'03) received the B.A.Sc., M.A.Sc., and Ph.D. degrees from the University of Waterloo, Waterloo, ON, Canada, in 1990, 1992, and 1996, respectively.

After completing his doctorate, he worked in the medical imaging field at Mitra Imaging Inc., Waterloo. He started his academic career in 1997 as an Assistant Professor in geomatics engineering at the University of Calgary. In 1999, he returned to the University of Waterloo as an Assistant Professor in systems design engineering and was awarded tenure and promotion to Associate Professor in 2003. He is an active interdisciplinary and multidisciplinary researcher and has a prestigious publication record, publishing refereed journal and conference papers in the diverse fields of remote sensing, computer vision, algorithm design, and biomechanics. His primary research interest is the automated interpretation of synthetic aperture radar sea ice imagery, in support of operational activities of the Canadian Ice Service. The research results have led to successfully commercial implementations.

Dr. Clausi has received numerous graduate scholarships, conference paper awards, and a Teaching Excellence Award.